IN-PLANE SHEAR PROPERTIES OF MULTIAXIAL 3D WOVEN COMPOSITE

Xinmiao Wang[1], Ling Cheng[2] , Li Chen[3] and Hui Guo[4]

[1] Key Laboratory of Advanced Textile Composites, Ministry of Education and Tianjin, Tianjin Polytechnic University, Tianjin, 300387, PR China. 347459518@qq.com
[2] Tianjin Polytechnic University, Tianjin, 300387, PR China. chengling@tjpu.edu.cn
[3] Key Laboratory of Advanced Textile Composites, Ministry of Education and Tianjin, Tianjin Polytechnic University, Tianjin, 300387, PR China. chenli@tjpu.edu.cn
[4] Red bean International Group, Wuxi, PR China. 846160349@qq.com

Keywords: Multiaxial 3D woven composites, In-plane shear properties, V-notches rail shear tests, Damage mechanisms, Failure modes

ABSTRACT

This paper evaluates the in-plane shear properties and damage mechanism of multiaxial 3D woven carbon/epoxy composites. Different multiaxial 3D woven carbon/epoxy composites and laminated composites were investigated using V-notched rail shear test. Comprehensive mechanical properties, such as shear strength, shear modulus, damage mechanisms and failure modes of multiaxial 3D woven composites and laminated composites were analyzed and compared. The effect of Z-yarn fineness, number of yarn layers and fiber volume fraction on in-plane shear properties of multiaxial 3D woven composites are also investigated. The comparison of in-plane shear properties of multiaxial 3D woven composites and laminated composites shows the existence of Z-yarns help make the better in-plane shear behavior of multiaxial 3D woven composites. The results also reveal that at the same thickness, as the number of yarn layers in the preform increasing, the maximum shear load increases. The specimen with coarser Z-yarn will bear the more shear stress, which is because coarser Z-yarns make bigger buckling-wave on the surface of perform to gather the warp yarns and ±bias yarns. And higher fiber volume fraction also helps improve the in-plane shear properties of multiaxial 3D woven composites materials. Moreover, the main failure modes of laminated composites included matrix cracking, fiber fracture, interfacial debonding and delamination, whereas the main failure modes of multiaxial 3D woven composites were significantly governed by Z-yarns and ±bias yarns, which can work together to help prevent the initiating and propagating of cracks, then help improve the ability of resisting shear deformation. These results presented in this paper serve as a baseline to further study the in-plane shear properties of multiaxial 3D woven carbon/epoxy composites.

1 INTRODUCTION

Via novel weaves recently developed, multiaxial 3D woven preforms, which include five yarn sets, +bias, -bias, warp, filling and Z-fiber, have been increasingly incorporated into various industrial sectors particularly in the field of civil and defense because of their excellent mechanical property, high stiffness and strength to weight ratio, and outstanding dimension stability.[1-5] As compared with laminated composites, 3D braiding composites and 3D orthogonal composites, a major advantage of multiaxial 3D woven composites is the obvious improvement in the in-plane shear properties caused by the addition of ±bias yarn. Hence, the mechanical responses of multiaxial 3D woven composites under in-plane shear load need to be systematically studied, and it is expected that a considerably enhanced properties can be exploited for a better design.

Ruzand and Guenot[6] developed a multiaxis 3D woven fabric based on lappet weaving principles, and there are four yarn sets, ±bias, warp and filling in this fabric. Anahara and Yasui[7-10] proposed another multiaxis 3D woven fabric, in which the normal warp yarns, weft yarns and bias yarns are held in place by the vertical binder yarns. Uchida et al.[11] developed a fabric called the 'five-axis 3D woven',

which consists of four layers and all layers are locked by Z-fibers. The sequences of the four layers are: +bias, -bias, warp and filling, from top to bottom. The tensile and compression results of this five-axis 3D woven composite were compared with stitched 2D woven laminate.[12] The results showed that the open hole tensile and compression results of this multiaxis woven structure were better than those of the stitched 2D woven laminated structure and the damaged area in terms of absorbed energy level was smaller in the multiaxis 3D woven composite. Mohamed MH and Bilisik AK[13-17] developed a multiaxis 3D woven fabric which has five yarn sets: ±bias yarns, warp yarns, filling yarns and Z-fiber. Many warp layers are positioned in the middle of the structure, ±bias yarns are positioned on the front and back face of the preform, and Z-yarns lock the other set of yarns. Some experimental studies were conducted on this multiaxis 3D woven composites and orthogonal 3D woven composites.[17] In-plane shear test results showed this multiaxis structure can enhance in-plane properties of the resulting composites due to the addition of the ±bias yarn on the surface of composites. There was a local delamination on the warp-filling yarns and local breakages on bias yarns through the thickness direction and surface of the multiaxis 3D woven composites for in-plane shear failure. However, bending experiment results and bending failure analysis indicated that the ±bias yarn orientations of multiaxis 3D woven composites cause a reduction in bending properties, whereas interlaminar shear test results showed that ±bias yarns have no considerable effect on interlaminar shear strength of the multiaxis woven composite. Ahmad Rashed Labanieh et al.[18] proposed a novel development to solve the issues related to the guide block technique, which is used to position the bias yarns in the weaving zone on the weaving loom. And geometrical characterization of manufactured preform, using the developed multiaxis 3D weaving loom prototype, has been carried out to observe the yarn geometry inside the impregnated preform.

However, although achievement has been made by scholars in researching multiaxial 3D woven composites, very limited researches are found in literature on this composite material in the systematic study of the behavior and damage mechanism under in-plane shear load which play a great role in the composite performance. This paper evaluates the in-plane shear properties and damage mechanism of multiaxial 3D woven carbon/epoxy composites. Different multiaxial 3D woven carbon/ epoxy composites (10 layers and 11 layers, both with two kinds of Z-yarn specification, 6K and 12K) and laminated composites ([+45/-45/0/90/0/90/0/90/-45/+45], [+45/-45/0/90/0/90/0/90/0/-45/+45]) were investigated using V-notched rail shear test. Comprehensive mechanical properties, such as shear strength, shear modulus, damage mechanisms and failure modes of multiaxial 3D woven composites and laminated composites were analyzed and compared. The effect of Z-yarn fineness, number of yarn layers and fiber volume fraction on in-plane shear properties of multiaxial 3D woven composites were also investigated.

2 EXPERIMENTAL DETAILS

2.1 Multiaxial 3D woven preforms

In multiaxial 3D woven perform, warp yarns and ±bias yarns are arranged in a matrix of rows and columns within the required cross-sectional shape, and the ±bias yarns can be oriented at ±θ° to each other at various positions: on the surface or in interior of the structure. Different position of ± bias yarns bring up the outstanding designability characteristic of multiaxial 3D woven perform. The structure of the multiaxis woven preform is shown schematically in Figure 1.

In this study, two kinds of multiaxis woven structures (10 layers and 11 layers) with ±bias yarns positioned on the surface of preform were newly developed. The two structures both have five sets of yarns: +bias, -bias, warp, filling, and Z-yarns. Warp yarn sets are longitudinally and filling yarn sets are placed transversely in matrix arrangements. +Bias yarn sets and - bias yarn sets are placed on both surfaces of the structure and +bias layers occupy the outermost part of the surface. Z-yarn sets lock all other yarn sets to provide the structural integrity.

The two kinds of multiaxial 3D woven preform in this study were made of T400 6K carbon fibers (Toray, Tokyo, Japan, the linear density is 400mg/m) and T700 12K carbon fibers (Toray, Tokyo, Japan, the linear density is 800mg/m). In general, the bias yarn specification is designed to be equal to that of –bias yarn. The specifications of the yarn sets and structural properties of multiaxial 3D woven performs are summarized in Table 1, Table 2 and Table 3, respectively.

2.2 Architecture of laminated preforms

The laminate performs studied were made of T700 12k carbon fiber plain cloth (areal density of 400 g/m^2, warp density and weft density are both 2.5 picks/cm) supplied by Toray. Table 4 summarizes the laminate composite characteristics.

2.3 Test specimens and procedures

These preforms were cut and placed inside the mold cavity (380×180×4mm). The resin system (JC—06A epoxy resin and JB-06 hardener were used at ratio 100:1, in weight) was injected into the mold at room temperature with the pressure was consisted of 0.4 mpa[19]. After infiltration, the resin was allowed to cure for 2h at 120℃ followed by post-curing for 3h at 80 ℃. The performance parameters of the material and resin are shown in Table 1. Figure 2 shows the schematic diagram of transfer molding techniques. Figure 3(a) and Figure 3(b) show the actual surface of multiaxial 3D woven composite and laminate composite, respectively.

The shear test of multiaxial 3D woven materials and laminated materials were conducted by SHIMADZU AG-250KNE universal material machine setup in the room temperature, as shown in Figure 4, following the ASTM D7078-12 standards[20-22]. The test specimens were cut from the molded plate from the manufactured composites and the edges were sanded in a polishing machine. The specimens were eccentrically loaded by the gripping fixtures and the loading generated a high shear stress at the center of V- notches (the specimen), and forced the specimen to fail along a nearly vertical shear crack. The load was applied through the universal material machine at a constant head speed of 2 mm/min. Resistance strain gauges were bonded along the middle line of V-notches at the angle of ±45° at mid-height on the surface of the specimen, to evaluate the shear strain during loading and until final failure. The applied load was 40N·m-50N·m and the strain data were collected by a Ws3811 Strain Collect System supplied by Beijing Wavespectrum & Science & Technology Co., Ltd. Six specimens families with symmerically located V- notches at the center were tested up to failure to determine the shear strength and to analysis the mode of failure. The details of the specimen for each test are list in Table 5.

The average shear strain is determined from the strain gauges using the relation:

$$\gamma = |\varepsilon_1| + |\varepsilon_2| \tag{1}$$

Where the ε_1 is the strain measured by the +45° guage and the ε_2 is the strain measured by the -45° guage. The average shear stress τ is then determined by dividing the applied load F by the area of the cross section between the notches.

$$\tau = \frac{F}{hb} \tag{2}$$

Where h and b are the dimension of thickness of specimen and width of V-notches with the unit is mm. The apparent shear modulus G is then calulated by dividing the average shear stress by the average shear strain.

$$G = \frac{\Delta\tau}{\Delta\gamma} \tag{3}$$

Where $\triangle\tau$ is shear stress increment with the unit is MPa, $\triangle\gamma$ is the shear strain increment which is relative to $\triangle\tau$.

3 EXPERIMENT RESULTS AND DISCUSSION

3.1 Shear behavior

The shear stress is calculated by dividing the applied load with the area of the notched section(See Equation (2)). The shear strain is determined from Equation (1) using the indicated normal strain of the ±45°strain gauges and the shear modulus is obtained using Equation (3). Table 6 presents

the results of V-notched rail shear test of all composites. The load × displacement curves for the V-notched rail shear tests is given in Figure 5.

Figure 5 (a) are curves of 10 layers composites and Figure 5 (b) are curves of 11 layers composites. It can be seen that curves of the two 10 layers and two 11 layers multiaxial 3D woven composites tested are approximately similar. The curves should show a typical linear response at a relatively low amount of shear load, but in reality, only the curve of W-10-12 specimen shows a linear response when the shear load is less than 6mm, then start to behave non-linearly with increasing displacement until final failure. While, other curves show a nonlinear response from the beginning to end. This could be because the specimen was not completely contacted with fixtures.

The initial slope of the six load ×displacement curves in Figure 5 (a) and (b) were large. Following increase of displacement, the shear load increase also, but when the displacement reach to some of extent, there are yield points in the load×displacement curves and then the shear load decreased quickly, probably implying that some fibers in specimen are pulled out, or even to be broken. With the displacement continue increasing , a decrease in shear load is observed after reaching the ultimate shear capacity, which can be due to the total shear failure of materials.

The multiaxial 3D woven composites showed higher strength than laminated composites with the same layer numbers. The 10 layers multiaxial 3D woven composites with 49.86% fiber volume fraction have higher strength value than 10 layers laminated composites with 55.56% fiber volume fraction. While, The 11 layers laminated composites has the highest 60.11% fiber volume fraction ,but its shear strength is lower than that of 11 layers multiaxial 3D woven composites, as shown in Figure 5 (b). This behavior on the one hand can be attribute to the absence of Z-yarns in laminated composites, which lead to the integrity of composite structure being poor, on another hand, when the fiber volume fraction being higher, the resin concentration in the interface of composites is lower, impacted the interfacial adhesion strength. When the composites are loaded, there is a lack of adhesive in the fracture surface of materials.

As can be seen, all of four kinds of multiaxial 3D woven composites show much higher modulus and shear strength than laminated composites L10 and L11, it illuminates the importance of Z-yarns existence on in-plane shear properties of composites. It also can be seen that, W-11-12 achieves the highest modulus of 12.67GPa followed by W-11-6, W-10-12 and W-10-6. The lowest modulus in multiaxial 3D woven composites exhibited by W-10-6, is 10.70GPa. The shear modulus of W-11-12 is 3% higher than W-11-6, and the shear modulus of W-10-12 is 1.88% higher than W-10-6. As two common fabric architectures, it is expected that an increase of Z-yarns fineness of multiaxial 3D woven composites will cause an increase in the in-plane shear modulus, and it is the same for in-plane shear properties. This phenomenon indicates that Z-yarns fineness is one of the factors that governs the in-plane shear properties in multiaxial 3D woven composites, which may owing to the fact that coarser Z-yarns make bigger buckling-wave on the surface of perform to collect the warp yarns and ±bias yarns. In addition, the composites with 12k Z-yarns has higher fiber volume fraction of than the composites with 6k Z-yarns.

It can also be seen from Table 6 and Figure 5 (d) that, in the case of laminated composites, 10 layers composites L10 has lower shear strength (130.69 MPa) than 11 layers composites L11(136.74 MPa) which may be caused by the higher fiber volume fraction in 11 layers composites(60.11%). It can be concluded from the comparison of 10 layers and 11 layers multiaxial 3D woven composites that, materials with 11 layers have better shear properties than materials with 10 layers (Figure 5 (c)). W-10-6 and W-10-12 show 6.88% and 7.39% lower shear strength than W-11-6 and W-11-12, respectively, which is attributed to the effect of fiber volume fraction and number of interweave points on in-plane shear properties in multiaxial 3D woven composites. The fiber volume fraction of 11 layers composites are both higher than 10 layers composites, which corresponds to the addition of number of yarns at load directions in unit cross-section of materials. On the other hand, the number of interweave points increases with the increasing of layers number. The number of interweave points of 11 layers multiaxial 3D woven composites is 9.09% more than 10 layers woven composites, and the interweave points in the composites guarantee the stability of composite materials to some degree.

Figure 6 presents the shear modulus of multiaxial 3D woven composites varied in the following order: W-10-6< W-10-12 <W-11-6 < W-11-12. Obviously, in comparison with W-11-6, W-10-12 and W-10-6, W-11-12 has the highest fiber volume fraction of 55.46%, and it exhibits a highest shear

modulus at 12.67GPa, and followed by the W-11-6 fiber volume fraction of 53.55% and W-10-11 fiber volume fraction of 51.45%, whereas W-10-6 has the lowest fiber volume fraction of 49.86%, and it exhibits the lowest shear modulus at 11.70GPa. This showing that fiber volume fraction is a very important parameter influencing the in-plane shear properties and higher fiber volume fraction help improve the in-plane shear properties of multiaxial 3D woven composites materials.

3.2 Failure process

The failure mode of multiaxial 3D woven composites and laminated composites are shown in Figure 7.

The final failure mode are divided into two groups: a majority of specimens were not completely sheared and others were completely sheared. Compared with laminated specimens, the presence of Z-yarns of multiaxial 3D woven specimens inhibit the development of cracks in the materials.

Cracking of 11 layers laminated composites is observed at a shear load of around 17 kN. A drop in the shear stiffness is then observed. The cracks of laminated composite materials initiated at ±45° direction and there are mainly ±bias yarns on the location of cracks. This shows that the in-plane shear properties are basically controlled by ±bias yarns. With increasing load, the shear failure becomes obvious due to the microcrack growth of the matrix. Furthermore, these cracks deflect at the fiber/matrix interface, leading to the generation of interface cracks, then these interface cracks further extended and connect to each other, giving rise to the materials failure. The failure mode of multiaxial 3D woven composites is similar with laminated composites, which also has yarns debonding and matrix debonding. Filling yarns at 90° direction which were perpendicular to the test direction broke and cracks propagate. While the cracks of ±bias yarns at ±45° directions extend at the yarn axial direction, and the cracks appear upon the surface of specimen. However, the existence of Z-yarns in multiaxial 3D woven composites prevent the crack propagation along the ±45° directions, therefore the fracture time of specimen will be postponed, which will increase the shear capacity of specimens under in-plane shear stress.

Figure 8 shows the fracture morphologies of multiaxial 3D woven specimen after in-plane shear test. Fracture occur between the adjacent warp yarns. The warp yarns at fracture surface are relatively complete and a majority of weft yarns are cut neatly. While, the fracture of some bias yarns show the broom-shaped. The analysis of fracture surface show cracks of specimen generated firstly at the regions between the external matrix of adjacent warp yarns and other yarns and these cracks further extend, then the warp yarns lose their carrying capacity, so shear load are bore all by weft yarns and ±bias yarns with lower fiber volume fraction. These two kind of yarns are been cut off finally, which means the specimen failure occured.

4 CONCLUSION

The in-plane shear properties of multilayer multiaxis woven composites and laminated composites were studied in this paper, and shear strength and shear modulus are obtained by calculation. Analysis shows that:

The comparison of in-plane shear properties of multiaxial 3D woven composites and laminated composites shows, the existence of Z-yarns help make the better in-plane shear behavior of multiaxial 3D woven composites, help prevent the initiating and propagating of cracks, and help improve the ability of resisting shear deformation.

The in-plane shear properties of multiaxial 3D woven composites are influenced by Z-yarn fineness, number of yarn layers and fiber volume fraction of preform. At the same thickness, as the number of yarn layers in preform increasing, the cross-sectional area of internal yarns increase, means the content of the resin decrease, which is tantamount to an increase of the number of yarns which bear the external stress in unit cross- sectional area of the materials , therefore the maximum shear load increases. Moreover, the specimen with finer Z-yarn will bear the less shear stress which is mainly because coarser Z-yarns make bigger buckling-wave on the surface of perform to collect the warp yarns and ±bias yarns.

The experimental results revealed that the V-notches rail shear test method according to ASTM 7078 can be used to test the in-plane shear properties of composites accurately and objectively, thereby it can provide an objective basis for the shear properties evaluation and production design of composites. However, in order to represent characterize the experimental data of in-plane shear properties of composite materials more accurately, it is necessary to enlarge the quantity of specimens to a certain degree.

REFERENCES

1. Mouritz AP, Bannister MK, Falzon PJ, et al. Review of applications for advanced three-dimensional fiber textile composites. *Compos A* 1999; 30: 1445-1461.
2. Beyer S, Schmidth S, Maidi F, et al. Advanced composite materials for current and future propulsion and industrial applications. *Adv Sci Technology* 2006; (50): 178-171.
3. King RW. *Three dimensional fabric material.* Patent 4038440, USA, 2006.
4. Kamiya R, Cheeseman BA, Popper P, et al. Some recent advances in the fabrication and design of three dimensional textile preforms: A review. *Composite Sci Technol* 2000; 60: 33-47.
5. Kadir Bilisik. Multiaxis three-dimensional weaving for composites: A review. *Textile Research Journal* 2012; 82(7): 725–743.
6. Ruzand JM and Guenot G. *Multiaxial three-dimensional fabric and process for its manufacture.* Patent WO 94/20658, International, 1994.
7. Anahara M and Yasui Y. *Three dimensional fabric and method for producing the same.* Patent 5137058, USA, 1992.
8. Yasui Y Anahara M, Omori H. *Three dimensional fabric and method for making the salne.* Patent 5091246, USA, 1992.
9. Yasui Y Anahara M, Hori F, Mita Y. *Production of three-dimensional woven fabric.* Patent Publication 05106140, Japanese, 1993.
10. Yasui Y Hori F, Ainano M, Takeuchi J. *Method and apparatus for production of Three-dimensional fabric.* Patent 5772821, USA, 1998.
11. Uchida H, Yamamoto T, Takashima H, et al. *Three dimensional weaving machine.* Patent 6003563, USA, 1999.
12. Uchida H, Yamamoto T and Takashima H. Development of low cost damage resistant composites. *Muratec Murata Machinery Ltd*, http://www.muratec.net/jp (2010).
13. Mohamed MH, Bilisik AK. *Multilayered 3D fabric and method for producin.* Patent 5465760, USA, 1995.
14. Bilisik K. *Multiaxial three dimensional(3D)circular woven fabric.* Patent 6129122, USA, 2000.
15. Kadir Bilisik. Multiaxis three dimensional(3D)fiat woven fabric and weaving methodFeasibility of prototype tube cartier weaving. *Fibres Text East Eur* 2009; 17: 63-69.
16. Bilisik K. Multiaxis 3D weaving: comparison of developed two weaving methods- tube-rapier weaving versus tube-carrier weaving and effects of bias yarn path to the preform properties. *Fibers Polym* 2010; 11(1): 104-114.
17. Bilisik K. Multiaxis 3D woven preform and properties of multiaxis 3D woven and 3D orthogonal woven carbon/epoxy composites. *J Reinf Plast Compos* 2010; 29(8): 1173-1186.
18. Ahmad Rashed Labanieh, Xavier Legrand, Vladan Koncar. Development in the multiaxis 3D weaving technology. *Textile Research Journal* ;2016, 86(17) : 1869–1884.
19. Zhang Guoli, Li Xueming. Optimal Design of Technological Parameters in RTM. Industrial textiles 2000; 6: 27-30.
20. Hui Gou. Meso-mechanical analyse of 3D multi-layer multi-axial woven fabrics. MA.Eng Thesis, Tianjin Polytechnic University, Tianjin, China, 2013.
21. ASTM D7078/D7078M-05. Standard test method for shear properties of composite materials by V-notched rail shear method. West Conshohocken: ASTM International. 2005.
22. Adams DO, Moriarty JM, Gallegos AM, et a1. Developments and evaluation of a V-notched rail shear test. In: *The 2002 SAMPE Technique Conference*, 2002, pp.59-71.

Figure captions:

Figure 1. Structure schematic diagram of the multiaxial 3D woven preform
Figure 2. The schematic diagram of transfer molding techniques
Figure 3. The actual surface of multiaxial 3D woven composites (a) and laminated composites (b)
Figure 4. V-notched rail shear test of multiaxial 3D woven composite and laminated composite
Figure 5. Load × displacement cures for specimens
Figure 6. Shear modulus of multiaxial 3D woven composites studied
Figure 7. Shear test process (a), failure mode of multiaxial 3D woven composite (b) and laminated composite (c)
Figure 8. Fracture morphologies of multiaxial 3D woven composites

Table captions:

Table 1 Performance parameters of raw materials
Table 2 Yarn parameters of four multiaxial 3D woven carbon performs
Table 3 Structural parameters of four multiaxial 3D woven performs
Table 4 Structural parameters of laminated composites
Table 5 Geometric parameters of woven specimens and laminated specimens
Table 6 In-plane shear properties of multiaxial 3D woven specimens and laminated specimens

Figures.

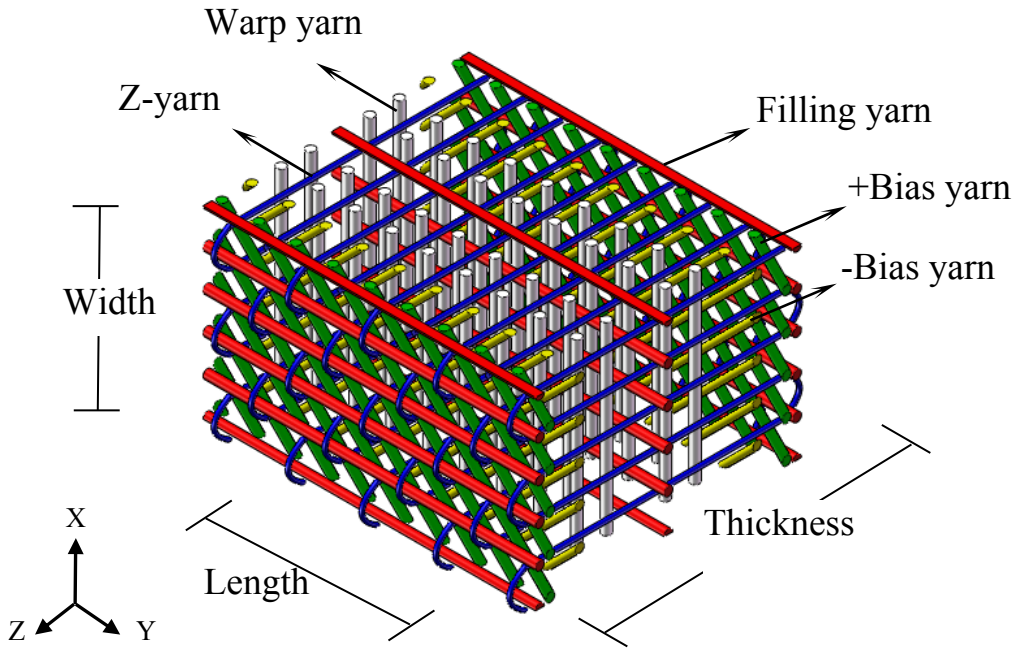

Figure 1. Structure schematic diagram of the multiaxial 3D woven preform

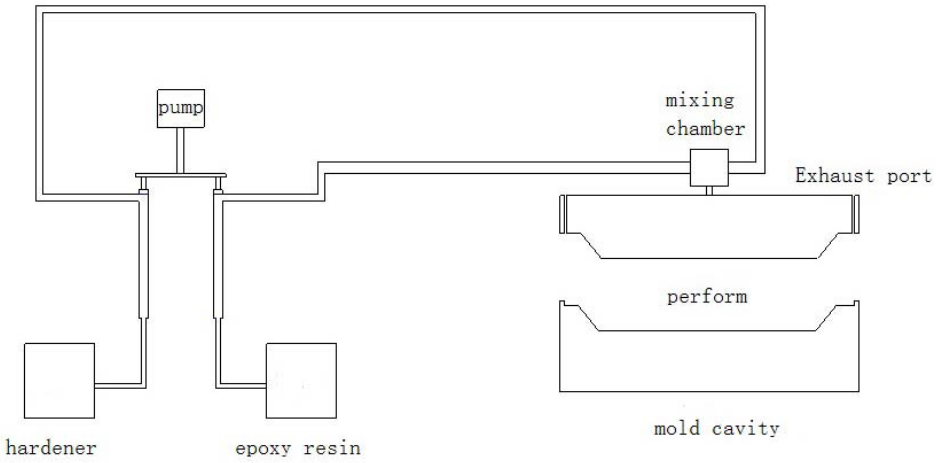

Figure 2. The schematic diagram of transfer molding techniques

(a) (b)

Figure 3.The actual surface of multiaxial 3D woven composites (a) and laminated composites(b)

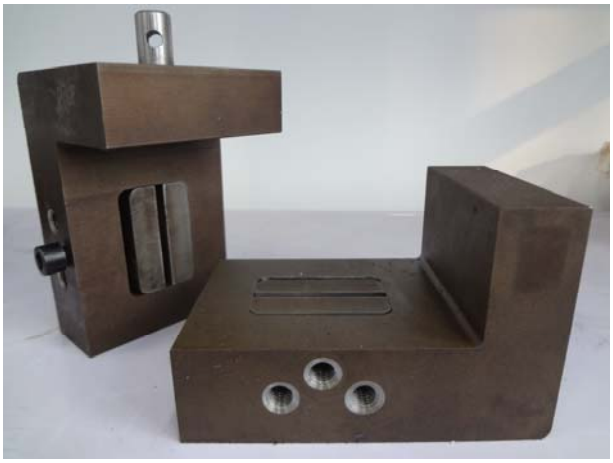

(a) test fixture

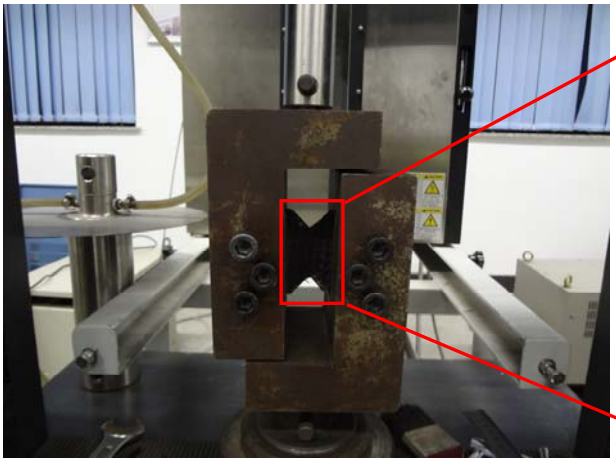

(b) test set-up

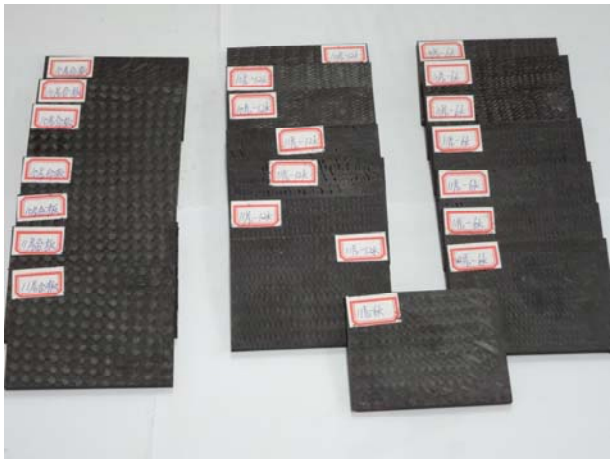

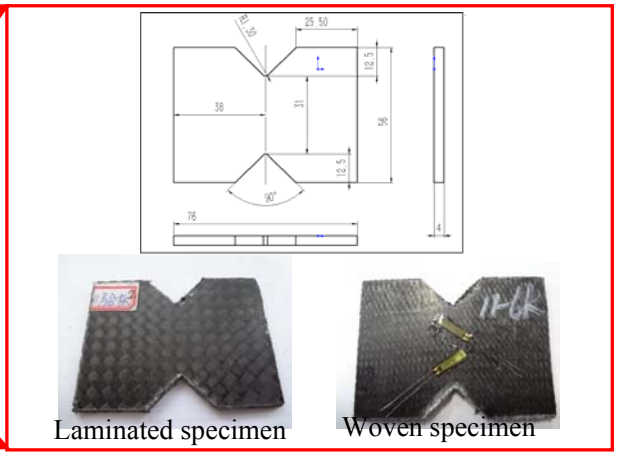

(c) specimens of multiaxial 3D woven composite and laminated composite

Figure 4. V-notched rail shear test of multiaxial 3D woven composite and laminated composite

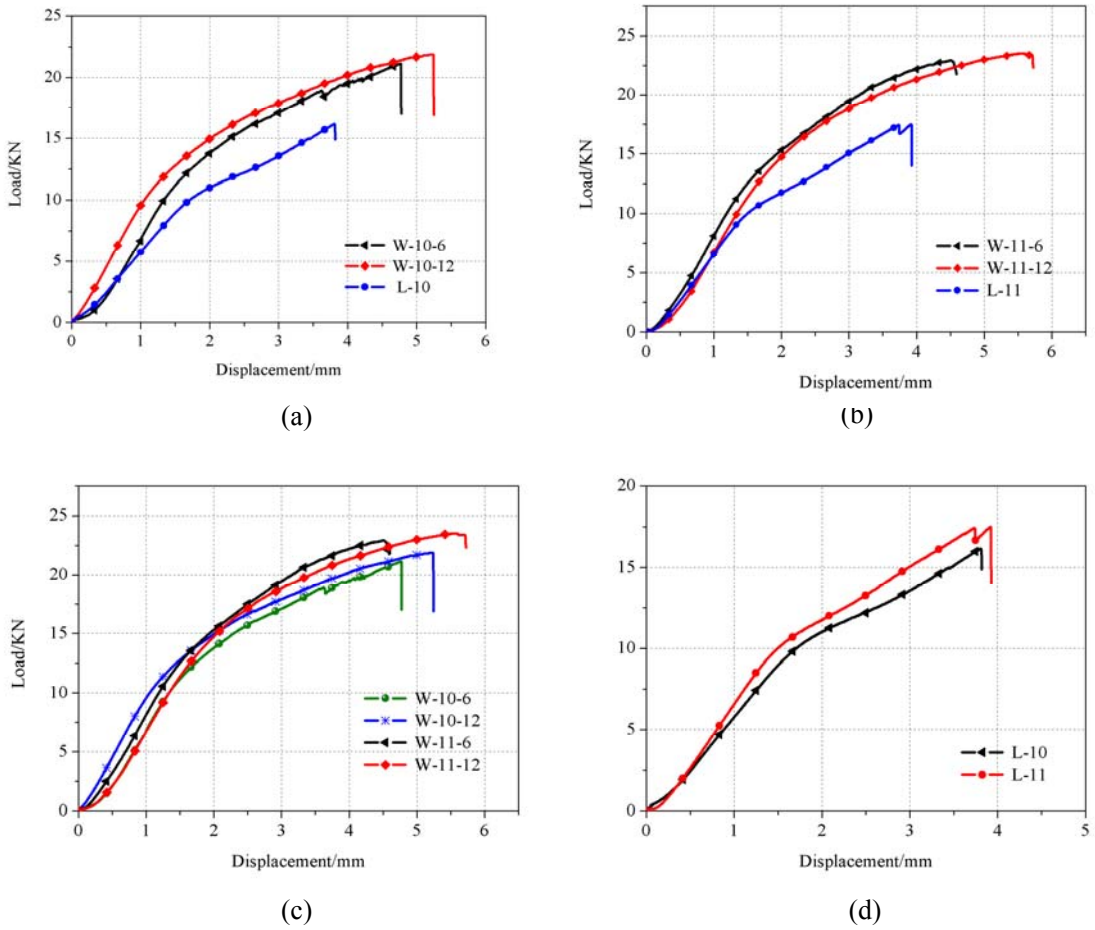

Figure 5. Load×displacement cures for specimens

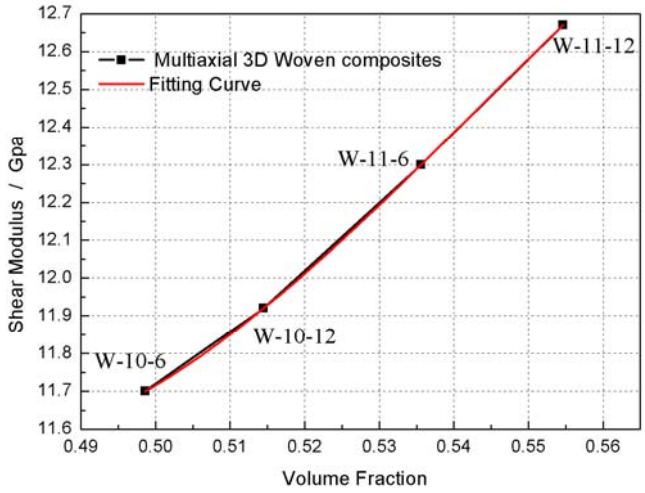

Figure 6. Shear modulus of multiaxial 3D woven composites studied

(a)

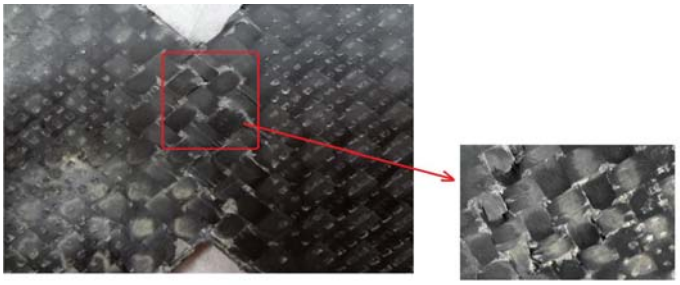

(b)

(c)

Figure 7. Shear test process (a), failure mode of multiaxial 3D woven composite(b) and laminated composite(c)

(a)

(b)

Figure 8. Fracture morphologies of multiaxial 3D woven composites

Tables.

Table 1 Performance parameters of raw materials

Raw material	Tensile strength MPa	Tensile modulus GPa	Density g/cm3	Elongation %
T400 6K carbon fibers	4900	230	1.8	2.1
T700 12K carbon fibers	4410	250	1.8	1.8
JC—06 epoxy resin	78.1	3.1	1.2	4.0

Table 2 Yarn parameters of four multiaxial 3D woven carbon performs

yarn linear density(mg/m)	yarn density((picks/cm))

warp yarns	weft yarns	±bias yarns	Z-fiber	warp density	filling density	bias density	Z-fiber density
800	800	800	398	4.4	4	4.4	4

Table 3 Structural parameters of four multiaxial 3D woven performs

families	linear density of Z-fiber	layer number	Thickness (mm)	order of arrangement	fiber volume fraction(%)	
					calculated value	measured value
W-10-6	6K	10	4.27	45/-45/0/90/0/90/0/90/-45/45	49.43	49.86
W-10-12	12K	10	4.41	45/-45/0/90/0/90/0/90/-45/45	51.02	51.45
W-11-6	6K	11	4.38	45/-45/0/90/0/90/0/90/0/-45/45	53.14	53.55
W-11-12	12K	11	4.47	45/-45/0/90/0/90/0/90/0/-45/45	55.08	55.46

Table 4 Structural parameters of laminated composites

families	layer number	Thickness(mm)	stacking sequence	fiber volume fraction(%)
L-10	10	4	+45/-45/0/90/0/90/0/90/-45/+45	55.56%
L-11	11	4	+45/-45/0/90/0/90/0/90/0/-45/+45	60.11%

Table 5 Geometric parameters of woven specimens and laminated specimens

specimen		specification	Z-fiber	Length(mm)	width(mm)	thickness(mm)	b(mm)
Laminates	L10-1	Ten layers	-	74.10	55.20	3.98	31.00
	L10-2	Ten layers	-	74.10	55.20	3.98	31.00
	L10-3	Ten layers	-	74.52	55.20	3.98	31.00
	L11-1	Eleven layers	-	73.64	55.10	3.98	32.00
	L11-2	Eleven layers	-	74.38	55.28	3.98	30.00
	L11-3	Eleven layers	-	74.62	55.36	3.98	31.38
Woven composites	W-10-6-1	Ten layers	6K	74.24	55.00	4.12	31.50
	W-10-6-2	Ten layers	6K	74.10	55.20	4.12	30.60
	W-10-6-3	Ten layers	6K	74.54	55.64	4.12	30.12
	W-10-12-1	Ten layers	12K	74.22	54.52	4.12	31.98
	W-10-12-2	Ten layers	12K	74.42	54.90	4.12	31.38
	W-10-12-3	Ten layers	12K	74.48	55.00	4.12	31.12
	W-11-6-1	Eleven layers	6K	74.20	54.80	4.00	31.68
	W-11-6-2	Eleven layers	6K	74.40	54.90	4.00	31.20
	W-11-6-3	Eleven layers	6K	74.70	55.18	4.00	31.60
	W-11-12-1	Eleven layers	12K	74.50	55.20	4.00	31.68
	W-11-12-2	Eleven layers	12K	74.12	56.34	4.00	31.14
	W11-12-3	Eleven layers	12K	74.10	55.08	4.00	31.44

Table 6 In-plane shear properties of multiaxial 3D woven specimens and laminated specimens

specimen	specification	fiber volume fraction(%)	Average In-plane shear strength (kN)	failure load(kN)	maximum stress(Mpa)	maximum shear strain	shear modulus (GPa)
Laminates	L10	55.56	16.19	16.19	130.69	0.02124	8.93
	L11	60.11	17.50	17.50	136.74	0.02157	9.54
Woven specimens	W-10-6	49.86	21.19	21.19	168.73	0.02456	11.70
	W-10-12	51.45	21.88	21.88	172.73	0.02115	11.92
	W-11-6	53.55	22.94	22.94	181.20	0.03241	12.30
	W-11-12	55.46	23.50	23.50	186.51	0.03982	12.67